Kilian *et al. Heritage Science* 2023, **11**(1):72
https://doi.org/10.1186/s40494-023-00900-z

Heritage Science

RESEARCH

Open Access

Investigation of the deterioration mechanisms induced by moisture and soluble salts in the necropolis of Porta Nocera, Pompeii (Italy)

Ralf Kilian[1,2*], Léo Borgatta[3] and Eberhard Wendler[4]

Abstract

This paper focuses on the diagnosis of damage processes of decorative Roman renders of a group of tombs in the Porta Nocera necropolis in the ancient city of Pompeii, Italy. Unprotected from various climatic events, the tombs keep on deteriorating since they were first excavated in 1954. Extensive on-site and laboratory diagnostics using non-destructive and low-destructive techniques have been able to demonstrate that soluble salts are among the major agents of deterioration, causing damage in the form of render delamination. Gypsum is formed on the surface of the materials by the deposition of sulfur dioxide, resulting in reduced porosity and hardening of the surface. Soluble salts of nitrates and chlorides that penetrate the tombs' masonry from the ground and are transported through the render layers tend to crystallize in subsurface. The crystallization—dilution cycles of the soluble salts cause major mechanical pressures, leading to the progressive destruction of the renders. Past conservation strategies to secure plasters have shown only limited effectiveness. In light of the data collected regarding salt decay, the authors propose new strategies, questioning the systematic use of grouts and restoration mortars for conservation treatments and focusing on preventive conservation and maintenance to ensure the long-term preservation of masonry and decorative surfaces of the tombs.

Keywords Diagnostic, Conservation, Archeological site of Pompeii, Porta Nocera necropolis, Decay, Soluble salts, Moisture Roman plaster, Methodology, Decorative surfaces

Introduction

Excavated during the 1950's by the archeologist Amedeo Maiuri and later during 1980's, the necropolis of Porta Nocera constitutes together with the necropolis of Porta Ercolano, one of the largest funerary complexes of the Roman city of Pompeii. The development of the necropolis extended over a hundred-year period, from the beginning of Pompei's time as a Roman colony in 80 BC until the eruption of Vesuvius in 79 AC that devasted the city [1]. Located outside the city walls, along the ancient road to Nocera, the necropolis was a prime location for the deceased to exhibit the wealth and social status they had acquired during their lives to travelers entering the city through the Gate of Nocera. Unlike the necropolis of Porta Ercolano, whose tombs belonged to illustrious characters of Pompeian society, that of Porta Nocera also holds the tombs of more modest citizens [2]. This particular feature of the necropolis of Porta Nocera contributes to the large variety of funerary architecture, from

*Correspondence:
Ralf Kilian
ralf.kilian@ibp.fraunhofer.de
[1] Fraunhofer-Institute for Building Physics, Holzkirchen, Germany
[2] Otto-Friedrich-University Bamberg, Bamberg, Germany
[3] Pompeii Sustainable Preservation Project, Holzkirchen, Germany
[4] Fachlabor für Konservierungsfragen in der Denkmalpflege, Munich, Germany

Fig. 1 Tomb PN-ES13. Picture taken in 1959. Courtesy of Stanley A. Jashemsky

Fig. 2 Tomb PN-ES13. Picture taken in September 2019

simple tombs with gravestones to vast funerary monuments richly decorated with burial chambers. Despite the development of the necropolis over a hundred years, and the fact that there were no strict rules in Roman funerary architecture, leaving the owners free to build their sepulture as they wished [3], the architectural landscape of the necropolis of Porta Nocera shows a surprising coherence. Lined up on either side of the Via de Nocera, the funerary monuments tend to imitate each other—the masonry of most of them originally covered with white stucco, embellished or not with fresco paintings.

Photographs taken during or shortly after the excavation of the monuments testify to the good condition of most of them, with stucco render covering large areas of their masonry (Fig. 1). Today, some tombs have lost up to 90% of their decorative surfaces and every year, hundreds of grams of original stucco come off the walls (Fig. 2). Damage to mural paintings and ancient renders can have many different and often interacting causes. In the field of conservation of porous building materials, besides microbiological attack [4, 5], soluble salts are considered to be among the most important agents of deterioration [6]. Many studies in the archeological site of Pompeii have highlighted the responsibility of soluble salts in irreversible decay of decorative surfaces [7–10].

Soluble salts and their devastating effects on building materials can be activated only with the presence of humidity and/or liquid water within the porous system [11].

Some salts are also able to absorb sufficient humidity from the atmosphere, i.e. they are deliquescent and are dissolved above a critical humidity. This fact explains their migration and displacement within the porous building materials [12]. With the changes in climate, cyclic processes of crystallization and dissolution will create mechanical pressure within the pore system of the original materials, causing mechanical damage [5].

Water and soluble salts can infiltrate porous building materials from different sources. Driving rain coming from the nearby coast can contribute to the transport of moisture and sea salts of chlorides within the tombs' masonry [13]. Ground water can infiltrate buildings by capillary rise. Recent research has shown the responsibility of capillary rise and rising damp in the deterioration mechanisms of decorative surfaces of some ruins of Pompeii [5, 14]. Ground water generally contains ions from different types of salts. In a burial complex like the necropolis of Porta Nocera, one can expect ground water to be enriched with nitrates, from the decomposition of organic materials [15]. Air pollution and especially sulfur dioxide (SO_2) can form acid deposition and conversion into sulfates. Since their excavation, the decorated surfaces of the ruins of Pompeii have been exposed to a polluted atmosphere [16]. Air pollution in the bay of Naples and/or ship traffic from the nearby sea is one source of SO_2 [17], but also volcanic emissions contain SO_2 [18]. The periods of volcanic activity coming from Mount Vesuvius overlooking the city of Pompeii may thus have contributed to acid deposition on the decorative surfaces of the ruins at the archeological site.

Finally, while salts may have originated from external sources, they can also be inherent in the masonry structures. For instance, terracotta bricks that were widely used in the tombs' masonry, if they are not properly fired may contain sodium sulfate, but also Portland cement presumably used in previous conservation measures on the tombs of Porta Nocera is well-known to contain soluble sulfates [19].

Considered the most precious part of a building, the decorated surface is not only the most exposed to deterioration and subject to damage and decay but also to modification and unsuitable, earlier conservation treatments [20]. Since the excavation of the site, there have been successive attempts to preserve the tombs' surfaces. Unfortunately, they were often poorly documented. At some point, also simple preventive measures have been implemented. Protective roof structures of different designs and materials have been built over some of the tombs and Plexiglass panels were erected on the front of two tombs. Remedial treatments, such as grouting, repointing of mortar and edging repair were carried out on the decorated surfaces of most of the tombs of the necropolis. Furthermore, some tombs have undergone partial reconstruction of masonry structures with concrete. Given the current precarious state of conservation of the decorative surfaces, many of the past conservation strategies seem to have failed to address the ongoing deterioration mechanisms. Some of the past conservation measures combined with a lack of site maintenance may even have amplified them.

This article focuses on the methodology used by the authors to diagnose the decorative surfaces from a group of tombs and discusses the results obtained, with the objective of providing a better understanding of the active mechanisms of physic-chemical deterioration induced by moisture and soluble salts that endanger the funerary heritage of one of the most important roman archeological sites in the world. This research is part of the Pompeii Sustainable Preservation Project (PSPP). Launched in 2012, under the direction of Fraunhofer-Gesellschaft and in association with research institutions in the conservation of built heritage, including the International Centre for the Study of the Preservation and Restoration of Cultural Property (ICCROM) and the Institute for Archeological and Monumental Heritage (IBAM, CNR) and in collaboration with the Parco Archeologico di Pompei (PAP), the PSPP has two main objectives: the long-term preservation of the funerary monuments of the necropolis, through research and the implementation of preventive conservation measures, and on the conservation and restoration of decorative renders that require urgent remedial treatments.

This study focuses on a group of four funerary monuments, representative of the construction technology of most of the tombs of the necropolis of Porta Nocera. Each of these monuments have undergone various conservation treatments in the past including those on the decorative renders carried out during PSPP's conservation campaigns in 2015 and 2018. This article also discusses the success of these interventions and the future to be given to conservation strategies in the necropolis of Porta Nocera.

Methods

Selected tombs

The tombs selected for this study are tombs PN-EN04, 06, 10, and 14. According to the nomenclature of the archeological site of Pompeii, PN = Porta Nocera; EN = North East. The group of tombs is located at the crossroads between the Via delle Tombe, parallel to the wall of the ancient city of Pompeii, and the Via Nocera, which leads to the city through the Gate of Nocera (Fig. 3).

The tombs are built of "plain" masonry, i.e., the masonry is filled with a mass of blocks of lava stone and lime mortar. The claddings of the tombs are composed of lava stones with corner chains of terracotta tiles (Fig. 4) and with the addition of travertine stones for the tomb PN-EN12. The joint use of stone and brick for the construction of masonry is called *opus mixtum*, a technique commonly observed on the monuments of Pompeii built after the establishment of the Roman settlement in the city in 80 BC [8, 21]. The surface of the lava stones that make up the claddings of the tombs is usually largely covered with lime jointing mortar that has been smoothed after application (Fig. 5). The tops of many tombs are covered by a protective layer of *cocciopesto*, i.e. a lime mortar to which, in addition to or instead of sand, fine shards of clay or fine fragments of brick with brick dust components are added. The time of this intervention is unknown to the authors but, according to archival photos, it dates from shortly after the excavation of the tombs.

The render that covered the facades is made of two preparatory layers—the *arriccio*—and a finishing layer—the *intonaco* (Fig. 6). The observations carried out under polarized light microscopy on the constitution of the render layers using thin-section of mortar samples from

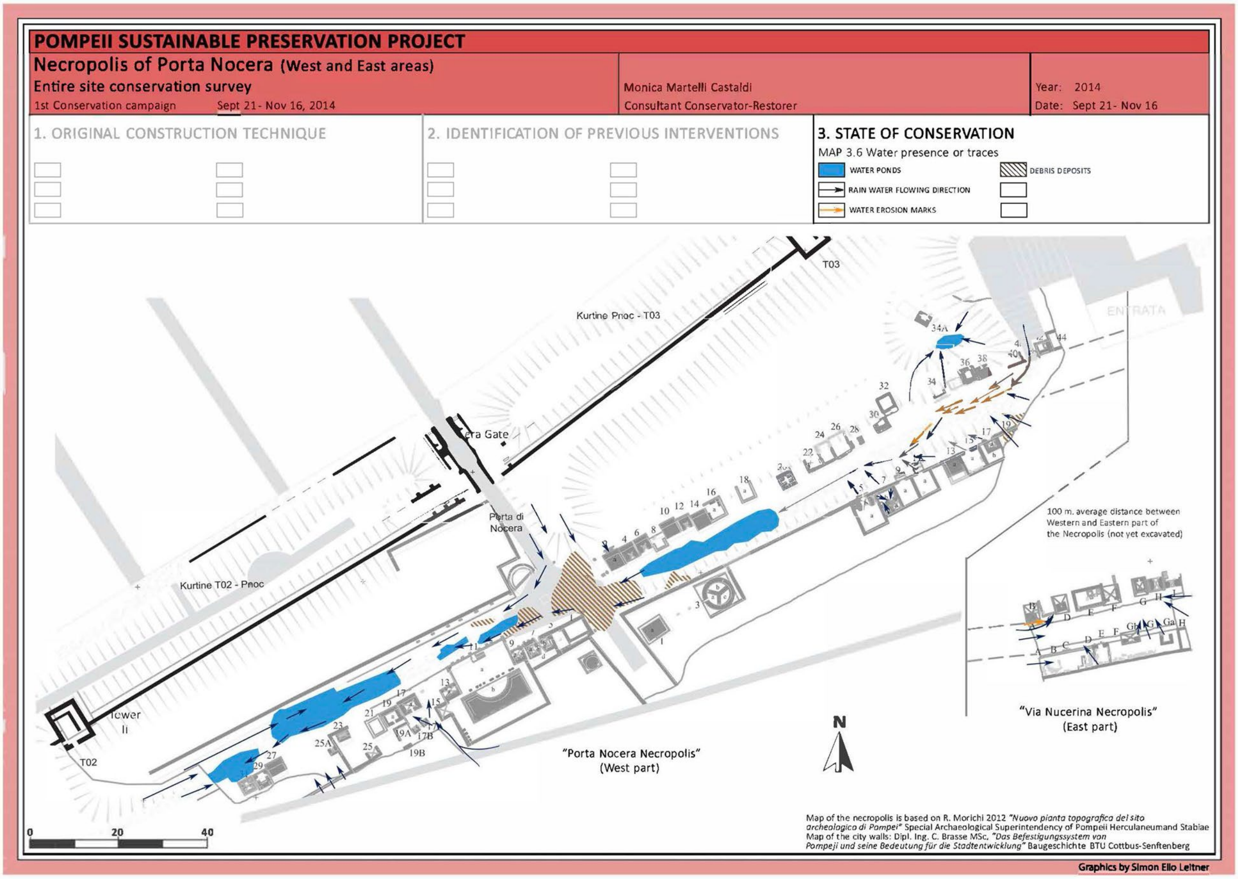

Fig. 3 Map of the path taken by rainwater in the necropolis and areas of possible stagnation according to observations on-site. The tombs selected for this study are frame in red. PSPP, 2014

tomb PN-EN04 and PN-EN06 showed that for all render layers, dry slaked lime was used as a binder. Air lime is considering to be the binder of render layers *arriccio* 0 and *intonaco*. Hydraulic reactions were identified in the mortar of the render layer *arriccio* 1 [22]. However, it is not clear if it is a natural hydraulic lime binder or if these reactions are of pozzolanic nature. The *intonaco* that imitates white marble blocks is composed of large aggregates of calcite crystals that give the surface a shiny effect. Both layers of *arriccio* are composed of aggregates of medium to well-rounded and polymorphic volcanic sands, minerals such as quartz or feldspars and a few carbonates. The high degree of rounding of the aggregates may indicate abrasion due to fluviatile or marine transport. Thus, river sands as well as coastal or beach sands of Pompeii's region can be considered as source material [22].

Decay in the render allows us to observe how the render layers were applied. The first layer of *arriccio* was often applied very coarsely to fill the irregularities of the masonry. By looking at the tool marks left on the surface of the mortar, it appears that the render layer was pressed against the wall using a trowel (Fig. 7). The pressure of the trowel brought the lime to the surface, leaving it binder-rich and smooth. The surface of the *arriccio* 1 render layer was applied in various thicknesses depending on the areas, from 1 to 4 cm. The surface of the *arriccio* 1 layer has generally been leveled with a float, to get a flat surface in preparation for the *intonaco*. Here too, the finishing work pulled the binder out and reduced the porosity of the surface.

Thin sections of render samples under a polarized microscope showed the systematic presence of sinter skins between the *arriccio* 1 and the *intonaco* render layer of the two tombs PN-EN04 and PN-EN06, which testify to an application of dry-on-dry mortar. This is also observed between the layers of *arriccio* 0 and *arriccio* 1 of tomb PN-EN04. The presence of sinter skins—thereby the application of successive layers of render on a dry substrate can reduce the adhesion between the layers, and the reduction of porosity induced by the sinter skins can decrease the permeability of the surfaces

Fig. 4 Tomb PN-EN10, west facade. Detail of the corner chain made of terracotta tiles disposed according to the "a vela" technique

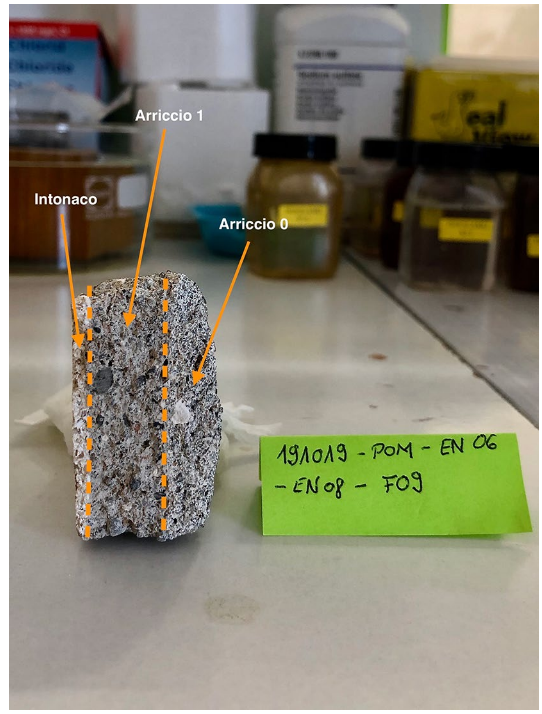

Fig. 6 Fragment of render collected at the base of tombs PN-EN06-08. The two preparatory layers of arriccio 0 and arriccio 1 and the finishing layer of intonaco can be distinguished

Fig. 5 Tomb PN-EN10, south facade. Detail of the lava stone cladding mostly covered by the lime jointing mortar

Fig. 7 Tomb PN-EN12, east facade. Detail of the surface of render layer arriccio 0. Traces of the working tools left after the application of the mortar are clearly visible

and reduce the transfer of liquid water between the render layers. The consequence of reduced water transfer will be discussed further in the results and discussion section.

Table 1 Characteristics of the different moisture meters selected to conduct the survey of moisture distribution in the facades of the tombs (according to manufacturer's technical description)

Devices	Depth of the measurements	Sensibility to soluble salts
Gann hydromette compact B	2–4 cm	Strong
Gann Hydromette UNI1 with active electrode B50	12 cm	Strong
Moist 2010 hf Moist R2 head sensor	7 cm	Low
Moist 2010 hf with Moist P head sensor	30 cm	Low

Dynamics of moisture and soluble salts transport in the necropolis

Located at one of the lowest points of the archaeological site, the necropolis acts as a "water tank" where rainwater that flows from the ancient city accumulates. The rainwater flows mainly from the three accesses which connect higher points of the ancient city with the necropolis, located to the east, west and north. The rainwater flowing from the ancient city usually stops at the lowest point of the necropolis, at the crossroads of the Via di Nocera (the street to the north that leads to the city through the Porta Nocera) and the Via delle Tombe (the road that crosses the necropolis from west to east). The survey on water flow carried out by the PSPP shown in Fig. 3 illustrates how water circulates and accumulates in the necropolis during rainy events.

Moisture and soluble salts transport dynamics in the tombs

Moisture and soluble salts distribution

In order to get first in situ data about moisture and soluble salt transport dynamics within the masonry of the tombs, two complementary non-destructive techniques (NDT) are selected:

Moisture meters aim at conducting a survey of moisture distribution in the tombs' structures. The selected device models rely on different technologies and allow moisture to be measured at different depths (see Table 1). According to the technology of measurements, the values measured may be more or less affected by the presence of soluble salts.

Passive infrared thermography is used to highlight the surface areas related to a certain range of evaporation rates. It can give complementary data as the moisture content of porous materials is strongly related to surface temperature. Enlargement of moisture near the surface will lead to a local decrease of temperature due to evaporation [23].

Used together with moisture meters that provide quantitative data on moisture distribution, passive IR thermography can be a helpful tool to support the analysis.

The survey using moisture meters was carried out in April 2019 and the survey using passive IR thermography at the end of September 2019. For both time periods, the measurements were taken in the morning, after a rainy night. The surfaces selected for the measurements are the north façade of tomb PN-EN 04 and the south façade of tomb PN-EN 14. The choice of these two measurement areas is justified by the desire to obtain comparative data between a south-facing and a north-facing surface, but also by the fact that both facades still present large square meters of complete rendering. Moisture meter data were taken in direct contact with the *intonaco*, yielding information for similar depths of the wall structure(s) for both facades. The data obtained for both moisture meters and passive IR thermography were converted into color scales in order to obtain comparative visualization maps.

Effective porosity and water transport properties

Effective porosity (i.e. the ratio of pore spaces accessible by fluids and gases), and water transport properties are key factors to understand moisture transport but also to assess the mechanical properties, the durability and the compatibility of the tombs' building materials [24].

The effective porosity of each single building material that constitute the tombs (terracotta brick, travertine stone, lava stone, bedding/jointing mortar, render layers) is measured in laboratory using the method of total immersion under vacuum according to standard DIN EN 1936:2006 [25] by testing material fragments collected at the bases of the tombs. This test method consists in defining the effective porosity of the material samples by means of their apparent and real densities. Apparent density (p_a) is the ratio of the mass to the apparent volume (volume including pore space) of the sample whereas real density (p_r) is the ratio of the mass to the real volume (apparent volume minus the volume of the pores spaces accessible to water)—both ratios expressed in kg/m^3 [26].

Real density is calculated by means of the following formula:

$$[p_r = \frac{M0 \times Dw}{M0 - Mw}]$$

And apparent density:

Fig. 8 Measurements of Water Capillary Uptake using Karsten Tubes in the arriccio 0 and arriccio 1 render layers

Fig. 9 Tomb PN-EN02. Measurements of Water Capillary Uptake using basin method in the cocciopesto protective layer

$$[p_{a=}\frac{M0 \times Dw}{Ma - Mw}]$$

where M_0 is the initial mass of the dry sample, M_a the mass of the water saturated sample in air, M_w the mass of the immersed sample in water and D_w the density of water at a given temperature (DIN EN 1936:2006).

Once real and apparent density are defined, the effective porosity (expressed in %) can be calculated by means of the following formula:

$$\phi(\%) = \left[1 - \frac{Pa}{Pr}\right] \times 100$$

The methodology of the measurement of the effective porosity according to standard DIN EN 1936:2006 is the following: the material samples are dried in an oven at 40 °C until they reach constant weight (M_0). The samples are then stored in a vacuum with a constant pressure of 20 ± 7 mbar (appx. 2 h) to remove the air from the pores. Deionized water is then slowly added to complete immersion of the samples. After 24 h, the saturated samples are removed from the water and surface liquid is wiped off using a wetted tissue. M_a is measured on a balance, followed by weighing under water (the sample fixed to the bottom of the balance) to measure M_w.

Fig. 10 Tomb PN-EN12, East facade. Measurements of. Water Capillary Uptake using Contact Sponges in the intonaco render layer

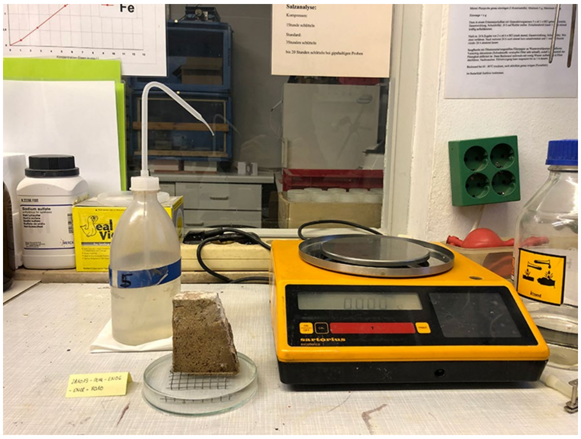

Fig. 11 Measurements of Water Capillary Uptake on a sample of terracotta tile, according to DIN EN 52617

Fig. 12 Measurements of Water Capillary Uptake on a sample of intonaco render layer, according to DIN EN 52617

A combined program of field and laboratory methods to define the water capillary uptake of the materials is set up. On-site, contact sponges method (CSM) and Karsten tubes (KT) are selected to measure vertical surfaces (Figs. 8 and 9) and impermeable basins for horizontal surfaces (Fig. 10). In laboratory, capillary water uptake measurements are carried out following the standardized test method DIN EN 52617 [27] on material fragments (Figs. 11 and 12).

CSM is able to measure the initial water uptake of dense material with high accuracy but it is not suitable for measurements over long periods and on highly porous materials, due to the limited water capacity of the sponge. On the other hand, KT has the capacity of measuring more porous materials with longer contact times [28]. Water basins on horizontal surfaces, constructed with the help of sanitary cement (i.e., long-term plastic material), are the least reliable method because it is difficult to produce an accurate contact area and water evaporation is not accounted for in absorption capacity measurements. Therefore, the results of these measurements should be taken with caution. They nevertheless give an approximate idea of the water uptake of the materials tested.

The Karsten tube (Fig. 8) has a graduated scale on its top. The open cylinder is fixed to the material surface using plasticine. Once fixed, the tube is filled with distilled water. Water uptake is measured versus time. The evaluation of the capillary water uptake coefficient (w-value) using KT is conducted by the computer program *Calkarow* [29]. This calculation program is based on the assumption of uniform, direction-independent liquid propagation in the porous structure according to capillary law regularity [30]. KT is used for measurements on arriccio 0 and arriccio 1 render layers (Fig. 8) as well as on volcanic stones from the tombs' masonry.

CSM uses a sponge contained in a circular contact plate. The diameter of the sponge corresponds to the inner diameter of the circular plate whereas the height of the sponge exceeds of a few mm that of the contact plate. For measurements, the sponge is filled with water and weighted together with the contact plate (w_0). The sponge (together with the contact plate) is pressed manually against the surface of the material to be measured until the edge of the contact plate touches the surface. The sponge is kept in contact with the surface of the material for 1 min, then removed and directly weighed again on the precision balance (w_e). The w-value of the material measured is calculated according to the following equation, where A equals the surface of the sponge of 0,002,376 m^2 [28].

$$w - value = \frac{w_0 - w_e}{A} \times t$$

CSM measures are carried out on the surface on the intonaco and on the dense surface of the mortar of the joints from the tombs' masonry. In order to obtain a set of comparative results, several surface areas on the different tombs are measured. Measurements are taken on surfaces considered to be in good condition, i.e. without cracks or asperities visible to the naked eyes.

Small basins of 25 cm^2 and 100 cm^2 using plasticine are created to measure water capillary uptake on horizontal surfaces of the tombs' construction materials. Measurements on horizontal surfaces are carried out to obtain data on the water uptake of the *cocciopesto* layer that should protect the top of the tombs to block rainwater infiltration (Fig. 9). As the *cocciopesto* layers presents deterioration patterns such as cracks and lacunas, measurements are also taken on horizontal surfaces of the underlaying construction materials of the tombs, namely bricks, lava stones, and pointing/jointing mortar. As stated before, basins method is the less reliable of the three test methods selected for water capillary uptake measurements. It gives however a rough idea of the water uptake of the different materials. The basins are filled with 100 ml of water (for basins of 25 cm^2) and 50 ml (for basins of 100 cm^2) until the water is completely absorbed, or, if not fully absorbed after an hour, the excess of water is removed and deducted from the initial water quantity.

As the curve of the water uptake (kg/m^2) versus time ($\sqrt{t}$) should be linear, the capillary uptake coefficient w can be calculated by the slope of the straight line, formulated by the following relation (31):

$$w\left[kg/m^2h^{0,5}\right] = \frac{m_w}{\sqrt{t}}$$

where m_w is the surface related water absorption (kg/m^2) and t is the absorption time (h)

Capillary water uptake measurements in the laboratory on samples from the tombs' building materials are conducted according to the standard DIN EN 52617 [27]. To obtain the best accuracy, the samples must have a regular shape with a defined soaking area. Thus, the edges of the material samples are cut using a grinder. For samples of decorative render, each layer—arriccio 0, arriccio 1 and intonaco is detached from each other to obtain separate results. The sample is positioned vertically on a metal grid, in a water filled glass container. After weighing the dry sample, its surface is brought into water contact, simultaneously starting a stopwatch. The sample is weighted on a precision balance at separate time intervals. Measurements end when the water has reached the top of the sample (Figs. 11, 12).

As for field methods of KT and basins, calculation method of water capillary uptake is based on the curve of the surface-dependent water absorption curve $\left[\mathrm{kg/m^2}\right]$ versus square time $\left[\sqrt{\mathrm{s}}\right]$ that is usually linear. The water uptake coefficient (w-value) is calculated by the slope of the straight line:

$$w\left[kg/m^2h^{0,5}\right] = \frac{m_w}{\sqrt{t}}$$

where m_w is the surface related water absorption (kg/m^2) and t is the absorption time (h)

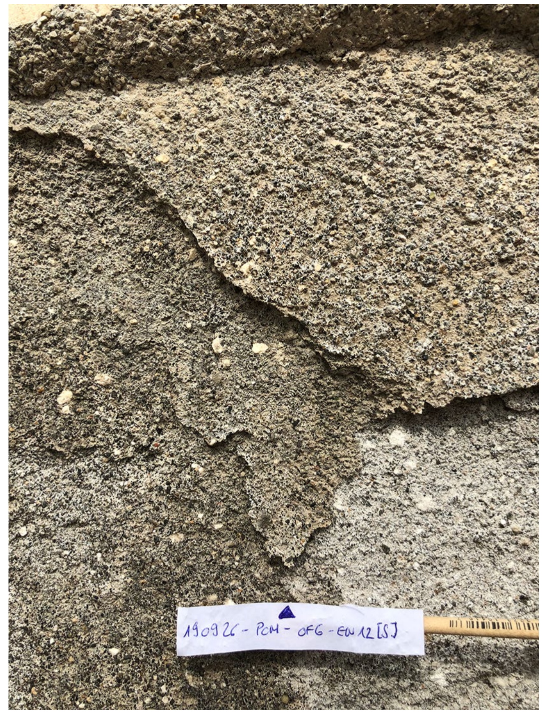

Fig. 13 Tomb EN12, south facade. Detail of the sampling area of the crust formed at the surface of the arriccio render layer

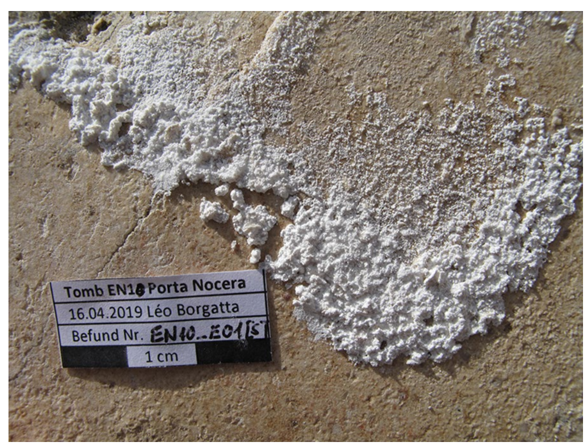

Fig. 14 Tomb EN10, south facade. Detail of the sampling area of soluble salt efflorescence on the surface of the intonaco render layer

Sampling of materials and soluble salt analyses

In order to get a better understanding of the salts that are causing damages to the ancient tombs, small material samples were taken for laboratory analysis. As seen in Figs. 13–14, different types of samples were taken:

- Efflorescence samples are taken on the south and east facades of tomb PN-EN06 (respectively on the surfaces of a brick and a volcanic stone), as well as in surface (Fig. 14) and sub-surface (behind a scale) of the *intonaco* on the west and south facade of tomb PN-EN14. The samples are qualitatively analyzing on-site using Merck® analytical strips and precipitation tests to get a first indication on the nature of salts in presence. The analyses are conducted directly on site (sampling time: April 2019).

Fig. 15 Tomb EN14, south facade. Area of sampling of powder material and of drilling resistance measurement using the apparatus DURABO®

- Drill powder samples are taken in several areas, chosen according to the degree of deterioration and the values given by the capacitance moisture meters. The drillings are undertaken with the use of a drilling resistance apparatus DURABO® with the aim of comparing the mechanical resistance of the material in relation to the quantitative salt load at different heights and depths (max 38 mm deep) in the south facade of tombs PN-EN14 and PN-EN06 and the north facade of tomb PN-EN04 (Fig. 15). The samples are qualitatively and quantitatively analyzed in laboratory by the determination of hygroscopic moisture content (HMC) according to standard ÖNORM B 3355 [32]; of electrical conductivity using a Hanna® HI 9033 device; and by the use a spectrophotometer DR600 UV–VIS from Hach®. The spectrophotometer allows to detect only the anions of the salt mixtures present in the samples. The analyses are conducted in the laboratory (sampling time: September 2019).
- Surface material samples are mainly taken from the weathering crust that has formed at the surface of render layers and masonry on the south facades of tomb PN-EN06, 10, 12 and 14 (Fig. 13). The samples are firstly visually analyzed under a Leica M205C microscope. The hygroscopic moisture content (HMC) according to standard ÖNORM B 3355 [32]. Semi-quantitative salt analyses are conducted using Merck® analytical strips and qualitative analyses are performed out by precipitation tests. The analyses are carried out in the laboratory (sampling time: September 2019).

Hygroscopic moisture content (HMC) is defined for drill powder and surface material samples according to standard ÖNORM B 3355 [32]. The test method aims at identifying of high moisture content—thus the presence of hygroscopic salts in the material sample. HMC values will allow the selection of samples for further quantitative analyses.

The test method consists in firstly weighting the samples as soon as they come to the laboratory. The samples are then dried at 60 °C until they reach constant weight (m_d). After drying, the samples are stored under constant relative humidity and temperature of 85% RH and 20 °C until they reach constant weight. Constant RH of the storage environment is reach thanks to a saturated solution of potassium hydrogen sulfate (K_2SO_4). HMC values are defined by the following equation:

$$\mathrm{HMC} = \frac{\Delta m}{m_d} \times 100$$

Were Δm is the mass gain by the sample and m_d the dry weight of the sample.

Electrical conductivity measurements (EC) are conducted with the device HI9033 from HANNA®. EC measurements gives a first indication of the whole ionic strength of samples' solution [33]. The dry samples are solubilized in 50 ml, 75 ml or 100 ml deionized water depending on their weight. As deionized water is not conductible an increase of conductivity values of the sample's solution is a signal of the presence of salt ions. Samples with high EC values are selected for further quantitative analyses.

Merck® analytical detection strips give ions concentration and pH values of the samples' solution according to the change in color of the test surface. Concentration values are given in ppm which corresponds to mg/l.

Precipitation tests are used as qualitative analyses to detect salt ions in the samples' solution. The principle of precipitation test is based on highly soluble compounds formed from clear salt solutions when brought in contact with ion specific reagents. By adding a few drops of an ion specific reagent, the intensity of the precipitation reaction can be qualified visually using a scale symbolized by (−) for no precipitation, (+) for low

Fig. 16 Tomb PN-EN14, south facade. Survey of moisture distribution using the device Gann Hydromette Compact B. Each range of value (in digits) corresponds to a color (see legend)

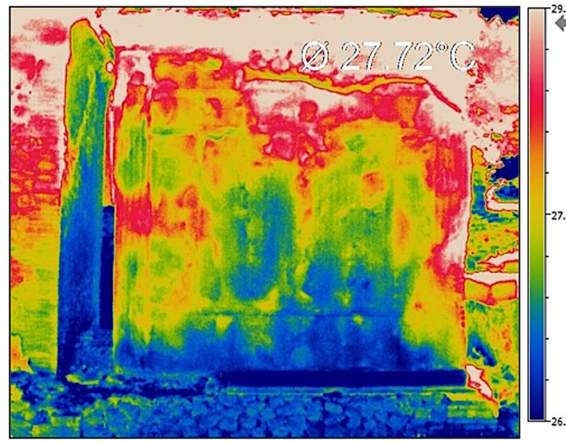

Fig. 17 Tomb PN-EN14, south facade. Survey of surface temperature distribution using passive IR thermography. The color scale in relation with temperature is given on the right side of the image

precipitation and (++) for intense and (+++) for very intense precipitation.

Quantitative tests are carried out using a spectrophotometer DR600 UV–VIS from Hach®. The spectrophotometer measures the level of intensity of the light absorbed after it passes through the sample solution, on the principle that every chemical compound absorbs or transmits light over a certain range of wavelengths. Thus, the concentration of ions in the solution can be determined by measuring the intensity of the light absorption of a specific ion complex or, as in the case of nitrate, by the absorption of the ion itself.

Results and discussion

In the following section the result from the in-situ analysis and laboratory research are presented and discussed.

Porosity and water transport

The survey of water transport dynamics in the necropolis of Porta Nocera has highlighted the areas where water stagnates during rain events. A large zone of stagnant water tends to form in front of the group of tombs selected for this study. This stagnant water can be detrimental to the conservation of the tombs because much of this water loaded with soluble salts must be absorbed by the ground and conducted into the foundations of the tombs, increasing the risk of salt transport in the masonries by capillarity. Signs of moisture supported salt transport by capillarity are highlighted by the investigation on moisture distribution in both tombs' facades combining moisture meters and IR thermography (Figs. 16, 17). The measures show the presence of two moist and salt loaded horizons in the southern facade of tomb EN14, located at dynamic equilibrium heights between 50 to 90 cm and 150 to 200 cm from the ground with an approx. overall height of the wall of 300 cm. Without the presence of soluble salts, the height reached by rising damp would oscillate in between 15 and a maximum of 100 cm. The fact that the salts are subject to deliquescence contribute to their mobility in the porous materials and increase the height of the capillary fringe [12]. Similar horizons are also clearly visible on other facades of the group of tombs where the masonry shows sanding deterioration linked to soluble salts activity.

With regard to the effective porosity and apparent density of the materials that constitute the masonry of the tombs (Fig. 18), results of the test show that there is great compatibility between the terracotta tiles, the jointing/bedding mortar and the travertine stone. All of these materials can be considered highly porous with effective porosity values of up to 37% for the tiles and for the jointing mortar and up to 44% for the travertine stone. Lava stone is by far the densest material in the masonry of tombs with an apparent density of 2490 kg/m^3 and an effective porosity of approximately 12%.

Concerning the render layers (Fig. 19), results show good compatibility between both *arriccio* layers with an effective porosity of approximately 36% and the tiles, jointing mortar and travertine stone in contact.

Greater differences in porosity values between the *arriccio* layers and the lava stones that make up the

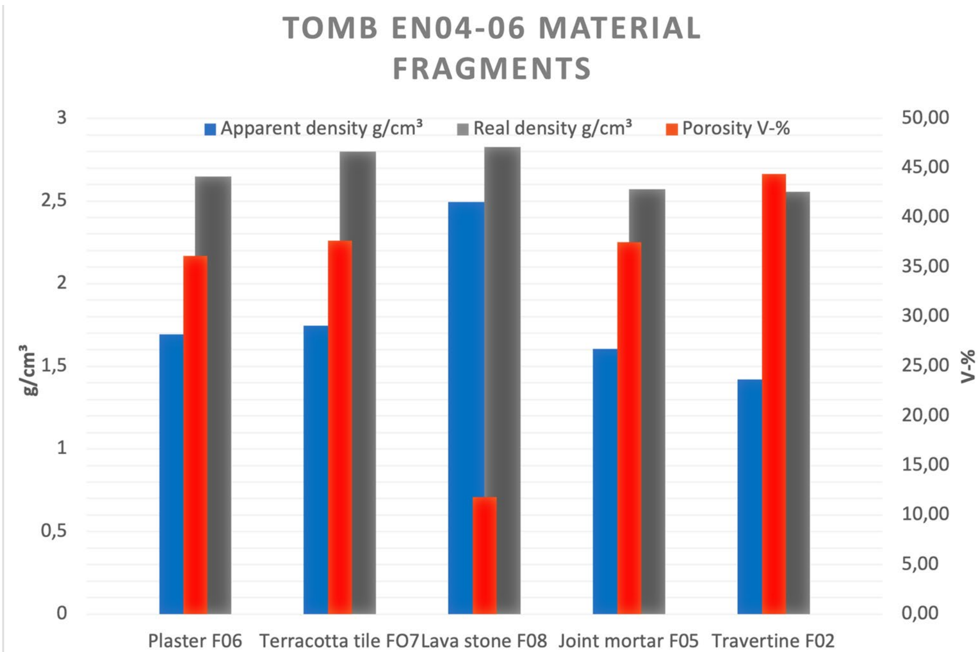

Fig. 18 Apparent density, real density, and effective porosity in relation to samples of material fragments

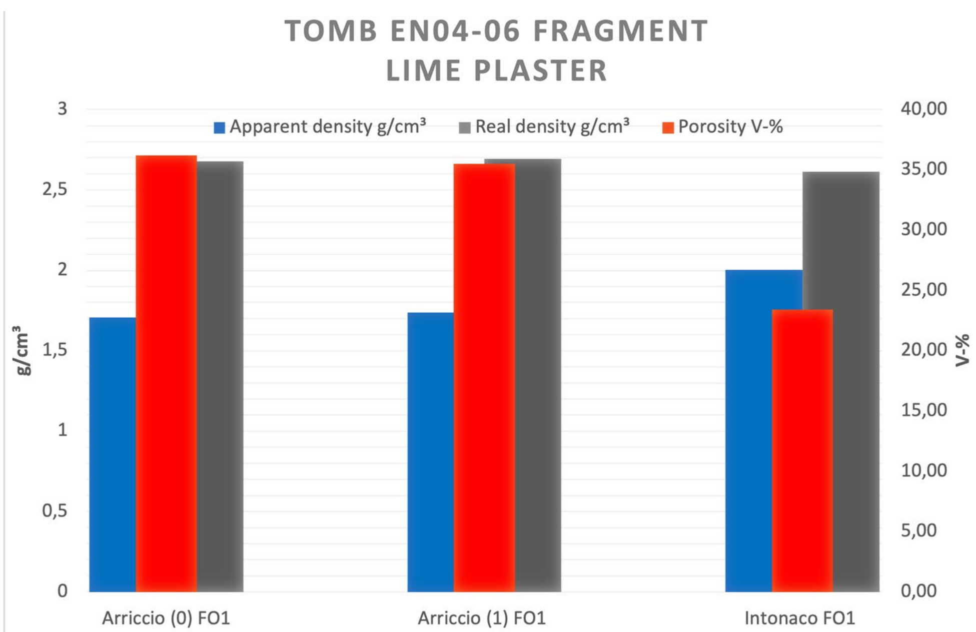

Fig. 19 Apparent density, real density, and effective porosity in relation to samples of render layers

facings of the tombs reflect a lower compatibility between the two materials.

The two *arriccio* layers have similar effective porosity values, while the *intonaco* is denser (2000 kg/m^3) and less porous (ca. 23%), but it can still be considered as a highly porous material.

While the effective porosity of building materials can give a first indication of the capacity of these materials to absorb water, this value is not sufficient to properly understand the water transfer system within such complex structures. The absorption capacity of a porous

Table 2 Results of Capillary Water Uptake coefficient-w of the tombs' building materials using on-site and laboratory measuring methods

Masonry	w-values on-site [kg/m^{2}h$^{0.5}$]		w-values laboratory [kg/m^{2}h$^{0.5}$]	
Methods	Basin	CS	KT	DIN 52617
Lava stone	6.1	–	2.8	–
Travertine	–	–	x	17
Brick/tile	9,1	–	–	14
Joint mortar	20	0,2–0,6	–	17
Cocciopesto	0,8	–	–	–
Render layers	w-values In-field [kg/m^{2}h$^{0.5}$]		w-values Laboratory [kg/m^{2}h$^{0.5}$]	
Methods	Basin	CS	KT	DIN 52617
Render layer Arriccio 0	–	–	11.9	17
Render layer Arriccio 1	–	–	4.3	12
Render layer Intonaco	–	0.1–0.7	–	9
Whole render system	–	–	–	19

KT Karsten Tubes, *CS* Contact Sponge, *Basin* in-situ measurement in area of horizontal surface

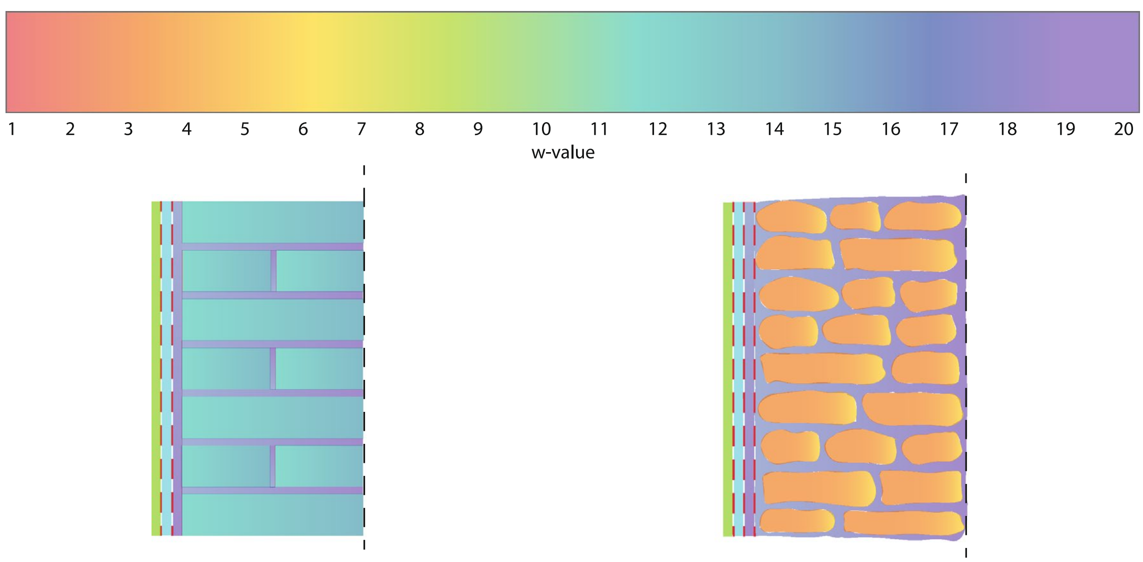

Fig. 20 Left: vertical section in brick masonry. Right: vertical section in lava stone masonry. The materials are colored according to the w-value. The red dotted lines indicate possible water transport barriers

material depends not only on its degree of porosity, but also and above all on the pores size distribution.

Regarding inorganic materials, the pore size can be classified in three categories: macropores (Ø > 1 mm); micropores (Ø = 0.1 mμ–1 mm); nanopores (Ø < 0.1 mμ). Micropores are mostly responsible for capillary water transport mechanisms [12].

The results of the measurements (Table 2) of water capillary uptake (w-value) of the tombs' building materials lead to the following conclusions (see schematic visualization of the water transfer system in Fig. 20):

- Rising damp, i.e. the infiltration of water on the masonries through the soil is facilitated by the hydraulic mortar used as bedding and jointing mortar for the lava stones, whose w-value is really high (17 kg/m^{2}h$^{0.5}$). The terracotta tiles used to build the corner chains (w-value = 17 kg/m^{2}h$^{0.5}$) of the tombs and the travertine stones (w-value = 14 kg/m^{2}h$^{0.5}$) will also highly contribute to the capillary rise of water in the masonry.
- The original render system, with the dense and polished surface of the *intonaco* layer (w-value between 0.1 and 0.7 kg/m^{2}h$^{0.5}$) provides a good protection for

the masonry of the tombs against the penetration of water from wind-driven rains. Nevertheless, for this protection to be efficient, the three-layers render system requires unity. As soon as deterioration (cracks, lacunas) in the *intonaco*'s surface exposed the really absorbent underlaying *arriccio* layers (w-value of the mortar mass of *arriccio* 0 = 17 kg/m^{2}h$^{0.5}$ and *arriccio* 1 = 12 kg/m^{2}h$^{0.5}$), a high quantity of water will be absorbed in a short time.

- The water capillary uptake measurements taken onsite show possible water transfer barrier at the interfaces of the render layers (red dotted lines in Fig. 20). This is suggested by the lateral spreading of the water when it reaches the underlying render layer. This lateral spread of water is due to the procedure of smoothing of the render layers, which has led to binder-rich and low porous surfaces. The same phenomenon is observed at the interface between the first preparing layer (*arriccio* 0) and the masonry of lava stones. This might be also due to the smoothing of the jointing mortar surface (w-value = 0.4 kg/m^{2}h$^{0.5}$) or the by the lower water absorption capacity of the lava stones (w-value = 2.8 kg/m^{2}h$^{0.5}$). Consequently, these water transfer barriers may lead to the accumulation of water between the render layers as well as at the interface between the render and the tombs' masonry in case of rain events. These interfaces may be preferential areas for the accumulation of soluble salts [34].
- The transfer of water between the masonry built up with travertine (EN_12) as well as with terracotta tiles (mainly corner chains of all tombs) and the preparing render layer (*arriccio* 0) should be allowed in both directions, i.e. from the masonry towards the render and vice versa, since all materials are in the same range of w-values.
- The *cocciopesto* layer that should protect the tombs from water infiltration from above seems to be effective thanks to its low w-value (0.8 kg/m^{2}h$^{0.5}$), but many gaps and cracks in the mortar most certainly reduce the effectiveness of this protection.

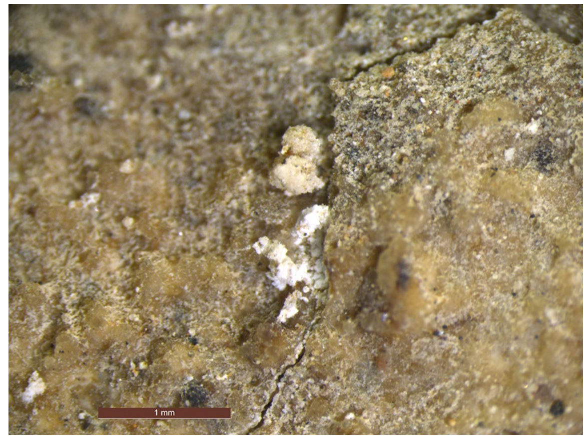

Fig. 21 Detail under microscope of the gypsum crust at the surface of a sample of a brick from the facade south of tomb PN-EN06. The surface is bulged and cracked. White salt crystals from subflorescence can be seen in the crack

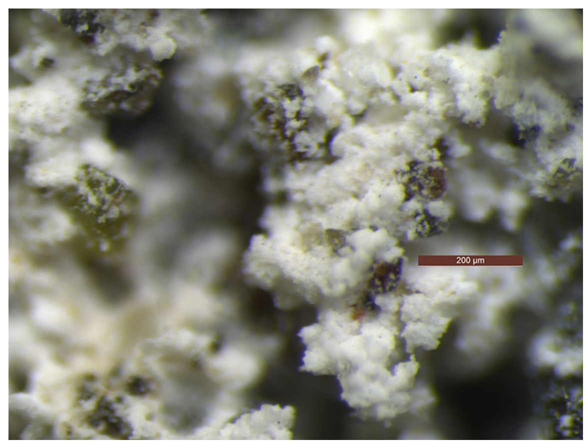

Fig. 22 Detail under microscope of white salt crystals at the backside of sample of brick material (same sample as Fig. 18)

Materials and soluble salts

Salt analysis provides a picture of the nature and distribution of soluble salts in the structure of the tombs.

The observations of the surface material samples under microscope systematically show a thin to a thick salt crust at the material surface and the presence of salt efflorescence at the backside (Figs. 21, 22).

The results of semi-quantitative salt analyses for the surface material samples confirmed the presence in high quantity of soluble nitrates and chlorides in the brick and joint mortar of the masonry. As seen in Table 3, soluble nitrates and chlorides are also detected in the material sample of the *arriccio* 1 render layer while only nitrates are found in the *intonaco*. Soluble sulfates appear in a lower concentration in all samples of surface materials. In situ qualitative sub-florescence analyses indicate the presence of sodium sulfate, a particularly damaging salt type.

The presence of high concentrations of sulfate anions and calcium cations (revealed by the semi-quantitative analyses of the salt crust from the surface material samples) indicates the formation of gypsum (Table 4), although the original, ancient render and masonry contained no gypsum, as confirmed by mortar analysis [22].

Table 3 Result of semi-quantitative salt analyses for the surface material samples solubilized in 2 ml demineralized water

Sample	Cl^-	SO_4^{2-}	NO_3^- [ppm]/(≃Wt.%)	Na^+	K^+	Mg^{2+}	Ca^{2+}	pH	HMC [Wt.%]
OF1 Brick	++	±	++	+	−	++	+	5.5	++
OF2 Joint mortar	++	±	++	+	−	++	+	5.5	+++
OF4 Intonaco	−	±	+++	+	−	+	+	5.5	±
OF5 Intonaco	−	±	+++	+	−	±	+	5.5	+
OF6 Arriccio 1	+	±	++	+	−	+	+	6.5	++
OF8 Grout (restoration)	++	−	++	−	−	++	++	6.0	+++

Table 4 Results of semi-quantitative salt analyses for the surface material samples solubilized in 15 ml demineralized water

Sample	SO_4^{2-}	Ca^{2+}	pH
OF1 Brick	+++	+++	5,0
OF2 Joint mortar	++	+++	5,5
OF4 Intonaco	+++	++	5,5
OF5 Intonaco	+++	++	5,5
OF6 Arriccio 1	+++	+++	7,5
OF8 Grout (restoration)	+	+	5,5

The salt load profiles given by the analyses of the depth powder samples taken directly in the masonry and the decorative render of the tombs confirmed the presence of sulfates at the materials surfaces. Soluble nitrates and chlorides are systematically detected in high quantity deeper in the masonry between 10 and 40 mm (Fig. 23). In contrast, only low concentrations of soluble nitrates and chlorides are found in the depth powder samples taken in the render layers. This, despite the fact that the render surfaces show deterioration typically related to soluble salts. The measurements of drilling resistance taken while sampling the material powder show systematically detachments between the render layers, even from the masonry and the *arriccio* 0 and/or between both preparatory layers of *arriccio* and/or between the *intonaco* and the *arriccio* 1.

With regard to these results and the observations of the deterioration patterns made on-site, it can be concluded that soluble salts are responsible for the partial detachment of the material surfaces in layers (delamination). The mechanisms that lead to this deterioration

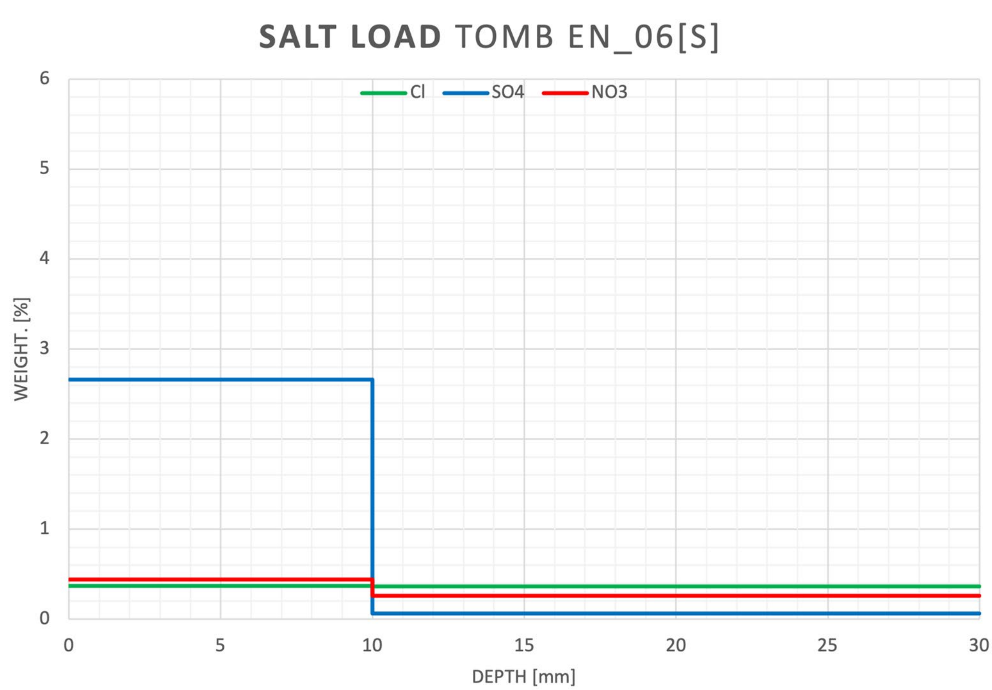

Fig. 23 Salt load for depth-profile S4 taken in a brick from the masonry of tomb PN-EN06, facade south

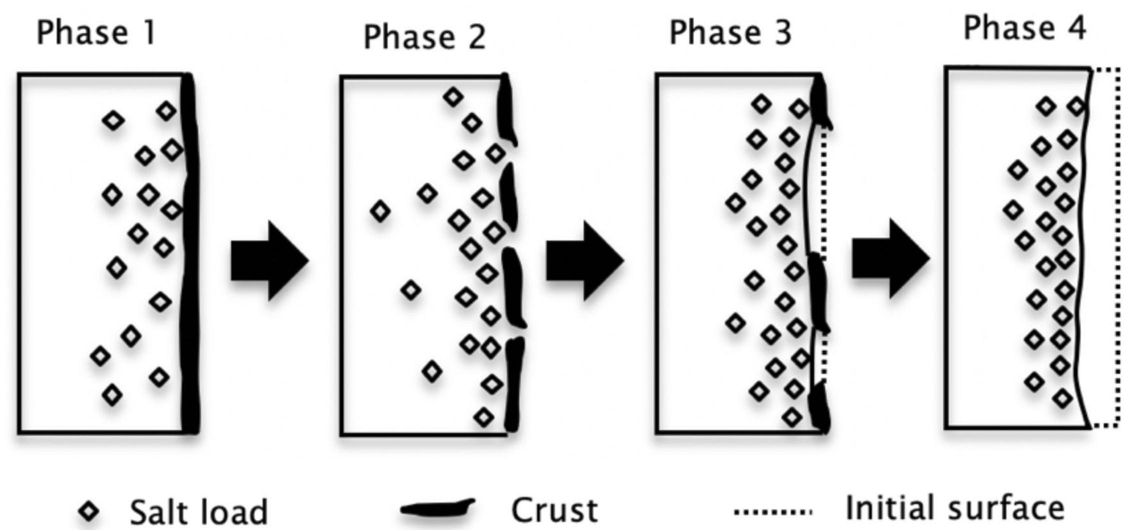

Fig. 24 Illustration of the successive phases of deterioration that lead to the partial detachment of the material surfaces

develop in several phases, graphically illustrated in Fig. 24.

In Phase 1, gypsum aggregates at the surface of the building materials in contact with the atmosphere. It is formed by the transformation of calcite ($CaCO_3$) contained in the joint mortars and renders into gypsum by dry or wet deposition (acid rain) of sulfur dioxide (SO_2). For this transformation to take place, two key characteristics are necessary [35]. First, moisture must be available at or near the porous surface. Second, there must be an oxidation reaction to convert SO_2 to sulfuric acid or to convert an intermediate sulfite salt to a sulfate (calcium sulfate dehydrate).

The gypsum accumulation can lead to hardened and denser surfaces [19], creating crusts which decrease the materials surface porosity [6]. With the formation of these crusts, the evaporation of moisture from the surface is reduced and consequently the risk of enhancing sub-florescence increases [24, 36].

In Phase 2, hygroscopic chlorides and nitrates penetrate the tombs from the soil and come up into the masonries by capillary rise and recrystallization. These salts tend to accumulate in two horizons, located approximatively between 50 and 90 cm and 150 cm and 250 cm from the ground (both horizons detected with NDT methods). However, most of these highly hygroscopic saline solutions might not cause noteworthy decay, as they would need an exceptionally dry climate for their crystallization [15]. On the other hand, non-hygroscopic sodium sulfate, certainly coming mainly from previous interventions containing cement, and accumulating as sub-florescence (Figs. 21, 22), can create high mechanical pressures underneath the surfaces while they go in and out of solution. Sodium sulfate is particularly damaging as it possesses two crystalline, solid phases: thenardite (Na_2SO_4) and mirabilite (Na_2SO_4 * 10 H_2O) [37, 38] The hydration pressure of the mirabilite is the most destructive since its molar volume is greater than that of thernadite. Sodium sulfate salt can increase in volume by more than three times when thernadite dehydrates to mirabilite [39]. The mechanical stress induced by changes in the hydration state of the crystalline salts leads to cracking, scaling and partial detachment of the surfaces.

In Phase 3, the accumulation of soluble salts in subsurface continues to cause surface detachment, leaving a more porous surface that has loss cohesion (sanding).

Phase 4 is the final state where the surface is completely gone, and the dissolution-crystallization and hydration-dehydration cycles of the soluble salts continue to proceed the granular disintegration of the material.

This process starting from the *intonaco*, consumes the render layers progressively and continue with the building materials of the tombs' masonry. The repetition of the process is made possible by the systematic reformation of the gypsum crust on the surface exposed to the atmosphere.

The phenomenon of delamination is especially to be observed on the tombs' facades oriented south, as they are particularly subject to strong variations in temperature and relative humidity due to their frequent exposure to the sun. Salt deterioration occurs during dissolution—crystallization cycles that take place under specified hygrothermal conditions that are specified from the salt mixtures in presence. Thus, large and fast fluctuations of

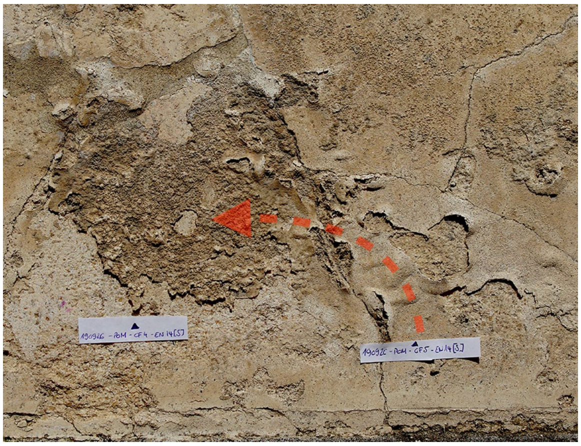

Fig. 25 Sampling area for samples OF4 and OF5, which shows significant deterioration by soluble salts. The red dotted arrow indicates the successive phases of transformation of the lime mortar surface into a gypsum crust

Fig. 26 Tomb PN-EN14, west facade. Detachment of the intonaco render layer from the arriccio with ca. 0.5 cm gap

relative humidity and temperature result in more damage than minor and slow fluctuations [6]. On the north facades the gypsum crust seems less likely to form.

The chemical conversion of calcite into gypsum can be easily observed on the surface area of the *intonaco* from the tomb EN14 southern facade. Here, the gypsum crust has not yet detached from the substrate and the surface area shows perfectly the transition of the healthy surface into a gypsum crust (Fig. 25).

Although the role of soluble salts in the delamination mechanisms that happen at the material surfaces is clearly defined, questions remain as to their contribution in the process of separation of the render layers from each other and from the masonry substrate. This mechanism of deterioration is another important issue for the stability of the render, as the layers can detach up to several centimeters (Fig. 26) and many areas of the render threaten to come off completely. As discussed above, the water transfer barriers observed at the interface between the render layers might be preferential zones for the accumulation of soluble salts and so for the deterioration of the mortar that would increase the detachment between the render layers. While the drill resistance measurements show systematic detachments between the render layers, the quantitative analyses of all drill powder samples taken through the detached render layers, show surprisingly low concentrations of soluble salts. These results have so far not been explained. One possible hypothesis would be that the voids created by the detachments inhibit the transport of soluble salts from the masonry through the successive render layers, concluding that grouting might accelerate decay in some areas. This should be a topic for further research.

Recommendations and further research

The approach of the PSPP to conservation is based on two precepts: the long-term preservation of the tombs through preventive conservation and the more immediate necessity to secure areas of render that risk detaching completely from the substrate through "first aid" remedial treatments. Remedial treatments should be limited to the most serious emergencies in order to gain time to think and to plan preventive conservation actions in combination with direct conservation interventions, such as cleaning, edge repairs, etc. which are carried out by the Parco Archeologico Pompeii. This is because a strategy that focuses on addressing the causes of deterioration is certainly "more effective, including cost effective than to attempt to strengthen against unrelenting inimical forces" [40].

Addressing the causes also means lowering the harmful effects of soluble salts. The conservation treatments carried out by the PSPP in its summer academies to secure the render by filling the voids with hydraulic grouting mortar and close the open edges of the render, have shown their efficacy but also their limits in the areas with high concentration of soluble salts. The monitoring of previous interventions shows that in a few restored areas where salts are prevalent, these irreversible interventions may have worsened the condition of the render.

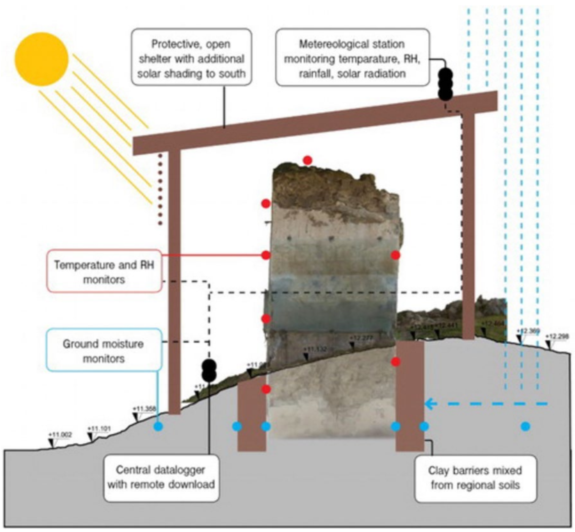

Fig. 27 Schematic of long-term monitoring and conservation strategy plan for tomb D-N. Courtesy of Michette et al. 2018 [6]

Fig. 28 Child playing on the ruins of the tombs of the Porta Nocera necropolis, Pompeii

One hypothesis is that re-bonding the render layers and the closing of open edges with lime mortar, establishing a new connection between the masonry and the render layers, will increase the transport of soluble salts through the render. This may accelerate the mechanisms of render detachment and delamination. However, further research is needed to confirm this assumption. More analyses of deep powder samples taken from areas where render layers were secured with grouting are needed, in order to gain more information on salt distribution within the grout and render layers. If the hypothesis of new connections between the detached render layers, giving a new path for soluble salts through the render, is confirmed, the systematic use of grouting and restoration mortar will have to be reconsidered and other reinforcement methods, for example mechanical reinforcement methods like clamps, may provide an alternative. This is a research topic to be further investigated.

Since the presence of liquid water is essential for any type of salt activity, preventive measures have to be considered. One important measure in order to slow down degradation is therefore to reduce the impact of water on the ancient structures. There are different options like building shelters [41, 42] or repairing the existing roofs and trying to prevent rising damp from the ground.

Research on preventive measures to preserve tombs from water intrusion and soluble salts have also been conducted in the framework of the PSPP, mainly on two aspects: the design of protective shelters[1] and the introduction of damp-proof barriers in the ground.[2] Tomb D-N located on the east side of the necropolis at the so-called Via Nucerina excavated in 1983 was selected for the implementation of preventive conservation measures. The tomb D-N is already protected by a simple shelter and damp-proof barriers made of natural clay still have to be placed at the base of the tomb. The protection system is equipped with several meteorological sensors to monitor temperature, relative humidity and soil moisture (Fig. 27). Once finalized, this system will provide data to better assess such conservation strategies, not only for Pompeii, but also for other archaeological sites.

For now, simple remedial and preventive measures could be implemented to prevent further degradation of the decorative surfaces of the tombs. Measurements of capillary water uptake on the *cocciopesto* that currently protects most the upper parts of the tombs from rainwater (recent restoration measure from the twentieth century) have demonstrated its low permeability. There are currently many gaps and cracks in this protective layer on most of the tombs that should be repaired with a mortar compatible with the original one. Tests on the properties and analysis of the original *cocciopesto* mortar will have to be conducted in order to develop a suitable repair mortar. This also applies to the deteriorated cornices of

[1] Together with researchers from Technische Universität München, see Fonti (41).

[2] Together with researchers from Fraunhofer Institute for Building Physics and Oxford University see Michette et al. (6).

the tombs that play a significant role in protecting the upper part of the tombs' facades.

The results of the diagnosis of the decorative surfaces of the tombs presented in this study highlights the vulnerability of the southern facades to ongoing deterioration mechanisms related to soluble salt activity. It is therefore crucial to protect the southern facades from direct exposure to the sun. The authors advise the use of movable and/or semi-translucent panels for shading. These panels could also serve as a means to inform visitors of the fragility of the decorative surfaces of the tombs (Fig. 28), as much anthropic damage in Pompeii could be avoided if visitors of the site were better informed about the vulnerability of the architectural surfaces [43]. The design of the panels and the materials to be used in their conception also need further research.

Finally, as the survey of water flow in the necropolis has shown, there are many areas on the Via delle Tombe where water stagnates, increasing the amount of infiltration of groundwater into the foundations of the tombs. Thus, it is essential to limit the moisture around the tombs by improving water management in the area. A simple measure would be to level the ground of the road regularly in order to avoid the formation of new breaches where rainwater could be trapped. More generally, the entire water evacuation system of the necropolis may benefit from a review.

If such measures can help to reduce the intrusion of moisture and soluble salts into the masonry of the tombs, they will not be sufficient to completely stop the deterioration caused by salts. This is because salts already present in the masonry are deliquescent. Therefore, with the fluctuations in relative humidity and temperature, which are almost uncontrollable in an outdoor environment, they will continue to move and exert mechanical stresses by moving from solution to solid. Thus, there is an urgent need for further research on salt reduction methods to extract salts from the masonries and to identify conservation measures which are durable in highly salt-laden monuments.

Conclusions

Through the use of non-destructive and less destructive test methods on site and in the laboratory, this study has highlighted the mechanisms of moisture and soluble salts on deterioration of decorative surfaces of a group of tombs from the necropolis of Porta Nocera. Gypsum is formed by the deposition of sulfur dioxide on the surface, resulting in reduced porosity and hardening of the surface. Soluble nitrates and chlorides penetrating the tombs' masonry from the ground are transported through the render layers causing damage by crystallizing in the subsurface. The crystallization—dilution cycles of the soluble salts cause major mechanical pressures, leading to the progressive destruction of the decorative renders. Therefore, special attention should be given to preventive measures to slow down the deterioration processes and new ways of securing delaminated plaster should be further investigated.

Abbreviations

PSPP	Pompeii Sustainable Preservation Project
ICCROM	International Centre for the Study of the Preservation and Restoration of Cultural Property
IBAM, CNR	Institute for Archeological and Monumental Heritage
PAP	Parco Archeologico di Pompei
NDT	Non-destructive techniques
CSM	Contact sponges method
KT	Karsten tubes
HMC	Hygroscopic moisture content
EC	Electrical conductivity measurements

Acknowledgements

The authors would like to thank Dr. Sara Saba from the Fraunhofer Institut für Bauphysik in Holzkirchen, Germany and conservator-restorer Julian James for their valuable suggestions and review of the text; Prof. Dr. Barbara Beckett from the Hochschule für Angewandte Wissenschaft und Kunst, Hildesheim, Germany and Prof. Monica Martelli Castaldi from the Università degli Studi Suor Orsola Benincasa, Naples, Italy for their scientific advice and assistance during on-site investigations; Benjamin Hübner and Suzanne Rother from the Fachlabor für Konservierungsfragen in der Denkmalpflege in Munich, Germany for their help with laboratory tests and analyses; Cornelius Palmbach from Bern University of the Arts, Switzerland for his advice on IR thermography; Prof. Massimo Osanna and Prof. Gabriel Zuchtriegel, former and present director of Parco Archeologico Pompei for providing us with the necessary authorizations to conduct on-site investigations.

Author contributions

The Pompeii Sustainable Preservation Project (PSPP) is led by the Fraunhofer Institute for Building Physics, Holzkirchen, Germany. Ralf Kilian is the corresponding author for this article (ralf.kilian@ibp.fraunhofer.de). This article stems from the research Léo Borgatta conducted for his Master thesis (01/20/2020) at Bern University of the Arts, Switzerland supervised by Barbara Beckett and Monica Martelli Castaldi in the context of the PSPP as directed by Ralf Kilian. Leo Borgatta participated in the 2018 campaign of the PSPP Project and since then has further investigated the topic in his master thesis, which is the basis for the submitted paper. Ralf Kilian is conservator and leads the PSPP project, which he co-founded in 2012 and has accompanied the research all the way. Eberhard Wendler is a chemist and conservation scientist and has contributed with his acknowledged expertise in the field of chemistry as applied to research and work in Cultural Heritage. All authors read and approved the final manuscript.

Author's information

Prof. Dr. Ralf Kilian is director of the Pompeii Sustainable Preservation Project. He teaches Heritage Conservation Science at Otto-Friedrich-University Bamberg, Germany, and coordinates the field of cultural heritage research at Fraunhofer-Institute for Building Physics, Holzkirchen, Germany. His research deals especially with aspects of building preservation and preventive conservation and is published in numerous publications on these subjects.
Léo Borgatta is a conservator-restorer of architectural surfaces from Lausanne, Switzerland. He graduated from the Bern University of the Arts with a Master in conservation-restoration. He is actually a research collaborator of the Pompeii Sustainable Preservation Project.
Dr. Eberhard Wendler is director of the Fachlabor für Konservierungsfragen in der Denkmalpflege. As a chemist, he is active in material science, construction chemistry and building physics, especially in the fields of stone decay and stone conservation as well as in aspects of harmful indoor climate. Besides more than 100 publications over a period of 35 years, he is concomitant of

many diploma- and masterworks at different European universities. He is the head of the WTA stone group.

Funding
Open Access funding enabled and organized by Projekt DEAL. This research was supported by Bern University of the Arts, Switzerland under the grant "Projektförderung Internationales".

Availability of data and materials
The datasets generated and/or analyzed during the current study are available from the corresponding author on reasonable request.

Declarations

Competing interests
The authors declare that they have no competing interests.

Received: 9 September 2022 Accepted: 5 March 2023
Published: 11 April 2023

References

1. Van Andringa W, Creissen T, Duday H. La nécropole romaine de Porta Nocera à Pompéi: naissance et développement d'un paysage funéraire romain (1er siècle av. J-C – 1er siècle après J-C). Chronique des activité archéologiques de l'École française de Rome. 2015. https://doi.org/10.4000/cefr.1528.
2. Pollone S. La necropoli di Porta Nocera Un percoso di memorie. In: Picone R, editor. Pompei Accessibile: Per una fruizione ampliata del sito archeologico. L'erma" di Bretschneider: Roma; 2013. p. 287–97.
3. Gros P. L'architecture Romaine. 2. Maisons, palais, villas et tombeaux. Paris: Editions A. et J. Picard. 2017.
4. Tonon C, Favero-Longo SE, Matteucci E, Piervittori R, Croveri P, Appolonia L, Meirano V, Serino M, Elia D. Microenvironmental features drive distribution of lichens in the House of the Ancient Hunt, Pompeii, Italy. Int Biodeterior Biodegrad. 2018;136:71–81. https://doi.org/10.1016/j.ibiod.2018.10.012.
5. Del Mondo A, Zuccaro G, Petraretti M, Pollio A, De Natale A. Water absorption coefficient drives *Nostoc* sp. colonization on mineral substrates. Int Biodeterior Biodegrad. 2021;164:105291. https://doi.org/10.1016/j.ibiod.2021.105291.
6. Charola AE, Blauer C. Salts in masonry: an overview of the problem. RBM. 2015;21(4–6):119–35. https://doi.org/10.1515/rbm-2015-1005.
7. Michette M, Bichlmair S, Kilian R. Diagnosing decay mechanism at the Porta Nocera Necropolis, Pompeii: the first step towards an effective preventive conservation. Stud Conserv. 2018;63:195–202. https://doi.org/10.1080/00393630.2018.1473197.
8. Pietro-Taboada N, de Fdez-OrtizVallejuelo S, Veneranda M, Marcaida I, Morillas H, Maguregui M, Castro K, De Carolis E, Osanna M, Madariaga J-M. Study of soluble salts formation in a recently restored house of Pompeii by in-situ Raman spectroscopy. Sci rep. 2018. https://doi.org/10.1038/s41598-018-19485-w.
9. Pérez MC, García Diego FJ, Merello P, D'Antoni P, Fernández-Navajas A, i Lacomba AR, Ferrazza L, Pérez-Miralles J, Baró JL, Merce P, D'Antoni H, Curiel-Esparza J. Ariadne's house (Pompeii, Italy) wall paintings: a multidisciplinary study of its present state focused on a future restoration and preventive conservation. Mater Construcc. 2013;63(311):449–67. https://doi.org/10.3989/mc.2012.00812.
10. Grifa C, Barba S, Fiorillo F, Germinario C, Izzo F, Mercurio M, Musmeci D, Potrandolfo A, Santoriello A, Toro P, Langella A. The Domus of Octavius Quartio in Pompeii: damage diagnosis of the masonries and frescoed surfaces. Int J Conserv Sci. 2016;7(2):885–900.
11. Doehne E. Salt weathering: a selective review. Geological society special publication natural stone, weathering phenomena. Conserv Strateg Case Stud. 2002;205:51–64. https://doi.org/10.1144/GSL.SP.2002.205.01.05.
12. Charola AE, Wendler W. An overview of the water-porous building materials interactions. RBM. 2015;21(23):55–65. https://doi.org/10.1515/rbm-2015-0006.
13. Traversetti L, Bartoli F, Caneva G. Wind-driven rain as a bioclimatic factor affecting the biological colonization at the archeological site of Pompeii, Italy. Int Biodeterior Biodegrad. 2018;134:31–8. https://doi.org/10.1016/j.ibiod.2018.07.016.
14. Madriaga JM, Maguregi M, De Vallejuelo SF-O, Knuutinen U, Castro K, Martinez-Arkarazo I, Giakoumaki A, Pitarch A. In situ analysis with portable Raman and ED-XRF spectrometers for the diagnosis of the formation of efflorescence on walls and wall paintings of the Insula IX 3 (Pompeii, Italy). J Raman Spectrosc. 2014;45(11–12):1059–67. https://doi.org/10.1002/jrs.4611.
15. Arnold A, Zehnder K. Monitoring wall paintings affected by soluble salts. In: Cather S, editor. The conservation of wall paintings. Los Angeles: Getty Conservation Institute; 1991. p. 103–35.
16. Maguregui M, Knuutinen U, Martínez-Arkarazo I, Giakoumaki A, Castro K, Madariaga M. Field Raman analysis to diagnose the conservation state of excavated walls and wall paintings in the archeological site of Pompeii (Italy). J Raman Spectrosc. 2012;43(11):1747–53. https://doi.org/10.1002/jrs.4109.
17. Murena F, Mocerino L, Quaranta F, Toscano D. Impact on air quality of cruise ship emissions in Naples, Italy. Atmos Environ. 2018;187:70–83. https://doi.org/10.1016/j.atmosenv.2018.05.056.
18. Carn SA, Fioletov VE, McLinden CA, Li C, Krotkov NA. A decade of global volcanic SO_2 emissions measured from space. Sci Rep. 2017;7:44095. https://doi.org/10.1038/srep44095.
19. Charola AE. Salts in the deterioration of porous materials: an overview. JAIC. 2000;39(3):327–43. https://doi.org/10.1179/019713600806113176.
20. Cianciolo Cosentino G, Kastenmeier P, Wilhelm K. Surfaces and environments. Introduction. In: Cianciolo Cosentino G, Kastenmeier P, Wilhelm K, editors. The multiple lives of Pompeii, surfaces and environment. Napoli: Prismi editrice politecnica; 2020. p. 9–11.
21. Adam J-P. La Construction Romaine. 5th ed. Paris: Editions A. et J. Picard; 2008.
22. Friedl C, Aichinger E. Der Wanddekoration der Grabbauten EN4 und EN6 der Nekropolis vor der Porta Nocera in Pompeji: Kombination von ausgewählten Mörtelanalysemethoden und Vergleich der Mörteleigenschaften. (Bachelor Thesis). Technische Universität München, Germany. 2016.
23. Grinzato E, Cadelano G, Bison P. Moisture map by IR thermography. J Mod Op. 2010;57(18):1770–8. https://doi.org/10.1080/09500341003731597.
24. Thomson M, Lindqvist JE, Elsen J, Groot C. Porosity of mortars. In: Groot C, Ashall G, Hugues J, editors. Characterisation of old mortars with respect to their repair. Champs-sur-Marne: RILEM publications; 2004. p. 75–103.
25. DIN EN 1936:2006. Prüfverfahren für Naturstein–Bestimmung des Wasseraufnahmekoeffizienten infolge Kapillarwirkung.
26. Teutonico JM. A laboratory manual for architectural conservators. Rome: ICCROM; 1988.
27. DIN EN 52617. Bestimmung des Wasseraufnahmekoeffizienten von Baustoffen. 1987.
28. Vandervoorde D, Cnudde V, Dewanckele J, Brabant L, de Bouw M, Meynen V, Verhaeven E. Validation of in situ applicable measuring techniques for analysis of the water adsorption by stone. Proced Chem. 2013;8:317–27. https://doi.org/10.1016/j.proche.2013.03.039.
29. Wendler E, Snethlage R. Wasseraufnahmeprüfer nach Karsten—Anwendung und Interpretation der Messwerte. In: Müller R, editor. Bautenschutz und Bausanierung 12. Köln: Germany; 1989. p. 110–5.
30. Meinhardt J, Zötzl M, Reicenbach C. Abschlussbericht zur Reparatur von Hochwasserschäden an der Skulpturen–Nachtrag zum Förderprojekt "Denkmalgerechte Betonindsetzung an den umweltgeschädigten Skulpturen Kuh und Pferd des bedeuten Bildhauers Gerhard Marks". Deutsche Bundesstiftung Umwelt. Osnabrück, Germany. 2014.
31. Siegesmund S, Dürrast H. Physical and mechanical properties of rocks. In: Siegesmund S, Snethlage R, editors. Stone in architecture. Berlin: Springer; 2011. p. 97–225.
32. Önorm B. 3355. Trockenlegung von feuchtem Mauerwerk—Teil 1: Bauwerkdiagnose und Planungsgrundladen. 2006.
33. Nasraoui M, Witold N, Lubelli B. A comparative study of hygroscopic moisture content, electrical conductivity and ion chromatography for salt assessment in plasters of historical buildings. Constr Build Mater. 2009;23:1731–5. https://doi.org/10.1016/j.conbuildmat.2008.09.029.

34. Groot C, Van Hees RPJ. Selection of plasters and renders for salt laden masonry substrates. Constr Build Mater. 2008;23:1743–50. https://doi.org/10.1016/j.conbuildmat.2008.09.013.
35. Grossi CM, Brimblecombe P. Effect of long-term changes in air pollution and climate on the decay and blackening of European stone buildings. In: Prirkyl R, Smith BJ, editors. Building stone decay: from diagnosis to conservation, vol. 271. London: Special Publication Geological Society; 2007. p. 117–31.
36. Modestou S, Theodoridou M, Ioannou I. Micro-destructive mapping of the salt crystallization front in limestone. Eng Geol. 2015;193:337–47. https://doi.org/10.1016/j.enggeo.2015.05.008.
37. Steiger M. Salts in porous material: thermodynamics of phase transitions, modeling and preventive conservation. Restor Build Monum. 2005;11:419–32. https://doi.org/10.1515/rbm-2005-6002.
38. Stahlbuhk A, Nissen J, Linnow K, Steiger M. Influence of the salt concentration on the damage potential of mirabilite and thernadite. In: SWBSS 2014, Third International Conference on Salt Weathering of Buildings and Stone Sculptures. 2014. https://www.saltwiki.net/index.php/SWBSS2014_Proceedings. Accessed 17 Nov 2022.
39. Doehne E, Price CA. Stone conservation: an overview of current research. Research in conservation. 2nd ed. Los Angeles: Getty Institute; 2010.
40. Cather S. Assessing causes and mechanisms of detrimental change to wall paintings. In: Rowing G, Heritage A, editors. Conserving the painted past: developing approaches to wall painting conservation. London: James & James; 2003. p. 64–75.
41. Fonti R. On the reading of the structural behavior of old masonry: The issue of the seismic assessment of archeological ruins. In: Theodore Simos (editor), International Conference of Computational Methods in Sciences and Engineering (ICCMSE 2016) Athens, 17–20 March 2016, vol. 1790. 2016. Conference Proceedings; 1300111–1300114. https://doi.org/10.1063/1.4968729
42. Laurenti MC. Research project on protective shelters for archeological areas in Italy A status report. Conserv Manag Archeol Sites. 2002;5(1–2):109–15. https://doi.org/10.1179/cma.2002.5.1-2.109.
43. Osanna M, Rinaldi E. Access and conservation at Pompeii: strategies for sustainable co-existence. Stud Conserv. 2018;63(sup1):203–18. https://doi.org/10.1080/00393630.2018.1495458.

Publisher's Note